JBUON 2016; 21(2): 390-398
ISSN: 1107-0625, online ISSN: 2241-6293 • www.jbuon.com
E-mail: editorial_office@jbuon.com

ORIGINAL ARTICLE

Personalized discovery of altered pathways in clear cell renal cell carcinoma using accumulated normal sample data

Xiaoyi Wang, Min Ding, Yong Yang, Yuehua Feng, Zhanqin Shi, Fengping Qiu, Ming Zhu

Department of Nephrology, The First Affiliated Hospital of Huzhou Teachers College, Huzhou 313000, Zhejiang Province, China

Summary

Purpose: *To identify altered pathways in an individual with clear cell renal cell carcinoma (ccRCC) using accumulated normal sample data.*

Methods: *Gene expression data of E-GEOD-40435 was downloaded from the ArrayExpress database. Gene-level statistics of genes in tumor and normal samples were computed. Then, the Average Z method was applied to calculate the individual pathway aberrance score (iPAS). Subsequently, the significantly altered pathways in a ccRCC sample were identified using T-test based on the pathway statistics values of normal and ccRCC samples. Moreover, the identified altered pathways were verified through two methods: one was assessing classification capability for microarray data samples, and the other was computing the changed percentage of each pathway in ccRCC samples.*

Results: *Based on the threshold, 886 altered pathways were identified in all samples. The most significant pathways were potassium transport channels, proton-coupled monocarboxylate transport, beta oxidation of octanoyl-CoA to hexanoyl-CoA, antigen presentation: folding, assembly and peptide loading of class I MHC, and so on. Additionally, iPAS separated ccRCC from normal controls with an accuracy of 0.980. Moreover, a total of 5 significant pathways with change in 100% ccRCC samples were extracted including proton-coupled monocarboxylate transport, antigen presentation: folding, assembly and peptide loading of class I MHC, and so on.*

Conclusions: *iPAS is useful to predict marker pathways for ccRCC with a high accuracy. Pathways of proton-coupled monocarboxylate transport, and antigen presentation: folding, assembly and peptide loading of class I MHC might play crucial roles in ccRCC progression.*

Key words: *average Z method, clear cell renal cell carcinoma, differentially expressed genes, pathway analysis*

Introduction

Renal cell carcinoma (RCC) represents the most common malignancy arising from renal parenchyma [1], leading to about 63,920 newly diagnosed cases and 13,860 deaths in 2014 in USA [2]. To our knowledge, ccRCC is the most common histological form of RCC, which accounts for about 80% of all renal cancers [3]. Unfortunately, the 5-year survival rate is only 50-69% [4]. Moreover, ccRCC is resistant to chemotherapy as well as to radiotherapy [5]. Consequently, a better understanding of the underlying pathogenesis of ccRCC is very urgent to find new therapeutic interventions.

As reported, in addition to smoking, cystic kidney disease and hypertension, genetic and pathway alterations also might contribute to the occurrence and progression of ccRCC [6,7]. Zubac et al. [8] have indicated that extracellular signal-regulated kinase 5 exerts important roles in ccRCC via mediating angiogenesis and proliferation.

Correspondence to: Ming Zhu, MM.. Department of Nephrology, The First Affiliated Hospital of Huzhou Teachers College, No. 158 Guangchangqian Road, Huzhou 313000, Zhejiang Province, China. Tel: +86 0572 2023728, Fax: +86 0572 2039251, E-mail: zhejiangzhuming313@163.com

Received: 21/09/2015; Accepted: 08/10/2015

Another study has demonstrated that the expression of plasma membrane–associated β-catenin is downregulated and related with advanced ccRCC [9]. Hypoxia-inducible factors pathway as well as upregulation of VEGFR and PDGFR pathways have been demonstrated to play important roles in ccRCC pathogenesis, via angiogenesis of renal tumors and the mutations in von Hippel-Lindau syndrome [10]. Additionally, Pei and colleagues have suggested that increased IMP3 enhances the cell migration and invasion of ccRCC through activating NF-κB pathway [11]. However, the potential mechanisms for ccRCC progression are still not fully understood.

In 2013, Wozniak et al. [12] provided the gene profile data of E-GEOD-40435 who identified the differentially expressed genes (DEGs) between ccRCC and adjacent non-tumor renal tissues. Moreover, pathway analyses and DNA methylation status were conducted. However, current pathway analyses are principally focused on identifying altered pathways between cancer and normal control group, and are not fit for extracting the pathway aberrance which might occur in an individual sample. Moreover, the conventional aim of defining important biological knowledge is to analyzing the expression of thousands of genes. Fortunately, Ahn et al. [13] have provided a straightforward and novel way to identify the pathway aberrance of individual sample by comparing the expression data profile of an individual tumor sample with the accumulated normal samples to further calculate the individual iPAS. Additionally, this aim of defining significant pathways is to perform the analysis on a pathway level rather than analyzing the expression of genes in a brute-force manner. Complementarily, we used this method to screen the aberrance of the pathway in a ccRCC sample through comparing it with the accumulated normal samples which were utilized as a reference.

Herein, in the present study, iPAS method was implemented to screen the altered pathways in ccRCC. Firstly, individual analysis was carried out to calculate the gene-level statistics and pathway-level statistics by making use of the accumulated normal samples. Then, the significantly altered pathways in a ccRCC sample were identified using T-test based on the pathway statistics values of normal and ccRCC samples. The altered pathways screened above were verified through two methods: one was assessing classification capability for microarray data samples, and the other was computing the changed percentage of each pathway in ccRCC samples.

Methods

Gene expression data and pathway data

The expression profile numbered E-GEOD-40435 [12] using the platform of A-GEOD-10558-Illumina HumanHT-12 V4.0 expression beadchip was downloaded from the ArrayExpress database [14]. All the 101 pairs of ccRCC tumors as well as adjacent non-tumor renal tissue biopsies samples were acquired from Czech patients, which included 42 women and 59 men. Moreover, there were 47191 probe IDs in the E-GEOD-40435. Then, probe IDs with concentrated expression level were converted to gene symbols. Repeated genes of expression value in matrix were removed. Finally, 31,314 genes were obtained.

All biological pathways in humans were extracted from REACTOME pathway database (http://www.reactome.org/) [15]. We filtered out pathways of which gene set size was more than 100. Moreover, the pathways with the intersection of 0 between genes in pathway and 31,314 genes obtained in our study were also excluded. Among pathways in REACTOME database, 1022 pathways involving 5,181 genes remained according to the gene set size.

Individualized pathway analysis

Data pre-processing and gene-level statistics

In the current study, we utilized accumulated normal samples as a reference and calculated the expression level of genes via comparing one cancer sample with many accumulated normal samples based on robust multichip average [16]. Briefly, the genes in all the collected normal samples for the reference were one by one normalized to the reference, and mean value and standard deviation (SD) of the expression level were computed. For individual tumor samples, we carried out quantile normalization after combining the single tumor sample with all reference samples. Supporting the genes with multiple probes, gene expression level was exhibited through averaging probe expression level. Gene level statistics of each gene in an individual tumor sample was standardized according to the mean value and SD of the reference genes. The specific formula was:

$$Z_{ij} = \frac{T_{ij} - \text{mean}(N_j)}{\text{stdev}(N_j)}$$

where Z_{ij} represents the gene level statistics of each gene in an individual tumor sample; mean (N_j) is the mean value of j-th gene of normal sample; stdev (N_j) is the SD of the expression level of j-th gene of normal sample; T_{ij} is the expression value of j-th gene of an individual tumor sample.

Pathway-level statistics

The average Z method, a modification of existing pathway analysis techniques, was applied to calculate the iPAS in normal and tumor samples. In brief, the gene level statistics of all genes in each pathway were extracted and summarized. Then, the average of gene-level information was transformed into the pathway statistics of this pathway. That is:

$$iPAS = \frac{\sum_{i}^{n} Z_i}{n}$$

where iPAS stands for the expression status of a pathway, Z_i denotes the gene level statistics of i-th gene, and n is the number of genes belonging to the pathway.

Overall significance test of pathways

To analyze the changes of pathways in all the 101 pairs of ccRCC as well as the adjacent non-tumor renal tissue biopsies samples, Gitools [17] were utilized to build the cluster heat map of pathways. T-test was used for measurement of pathway statistics of each pathway in normal and tumor samples. All the collected normal samples for the reference were compared one by one with the reference to yield the null distribution of pathway statistics. Then, p value was generated, based on the comparison between the null distribution and a statistic of a single ccRCC sample. Moreover, the results of analysis were corrected for multiple hypothesis testing using the false discovery rate (FDR) control by Benjamini and Hochberg (BH). Pathways with a FDR adjusted p value of less than 0.01 were considered significantly different.

Validation of the altered pathways

In the current study, we used two methods to verify the identified altered pathways based on iPAS using the accumulated normal data. One was assessing the classification capability for microarray data samples. The other was computing the changed percentage of each pathway in ccRCC samples.

Classification capability for microarray data samples

In order to evaluate the classification capacity of the altered pathways obtained from our methods for microarray data samples, the hierarchical clustering analysis was conducted based on the top 10 altered pathways using Gitools [17]. Under ideal condition, the samples should be divided into two main clusters including ccRCC cases as well as normal controls. We measured the iPAS method by testing the percentage of test samples that could be correctly classified.

In an attempt to assess the classification performance of our approach, the term of accuracy was measured [18]. Accuracy is defined as the fraction of correctly classified samples over all samples.

$$\text{Accuracy} = \frac{TN + TP}{TN + FN + FP + TP}$$

where TP symbolizes the number of true positive samples correctly predicted as positive; TN represents the number of true negative samples correctly predicted as negative; FP devotes the number of false positive samples incorrectly predicted as positive; and FN stands for the number of false negative samples incorrectly predicted as negative.

Changed percentage of pathway

Significance was required against the null distribution produced from normal cases. Based on the distribution of pathway statistics of each pathway in normal samples, a pathway statistic from a single tumor sample was compared with the null distribution to yield p value. Then, the number of tumor samples in each pathway was obtained according to p value < 0.05. Thus, the ratio of tumor samples in specific aberrant pathway with p value < 0.05 to all tumor samples was received. In the current study, the remarkably aberrant pathways in all tumor samples were extracted based on the changed percentage of each pathway in all ccRCC samples = 100%.

Results

Brief outline of average Z method and overall significance test of pathways

The average Z method was used to analyze the pathways and assign to each sample c and pathway P a score iPAS(c), which evaluated the extent to which the behavior of pathway P deviated in sample C, from normal samples. To determine the iPAS of this pathway, we applied the expression levels of all genes belonging to pathway P, using accumulated normal samples as a reference.

After the gene-level statistics of genes was transformed into the pathway-level statistics value of each pathway, T-test was used for the measurement of pathway statistics of each pathway in normal and tumor samples. Moreover, FDR approach was applied to correct significance levels (p values) for multiple hypothesis testing. Based on the FDR<0.01, 886 pathways were identified in ccRCC and normal samples. Subsequently, the cluster analysis was performed to explore the changes of the 886 pathways. The cluster heat map of these 886 pathways is shown in Figure 1. More importantly, these pathways were ranked in ascending order on the basis of FDR, and the top 10 significant pathways are exhibited in Table 1.

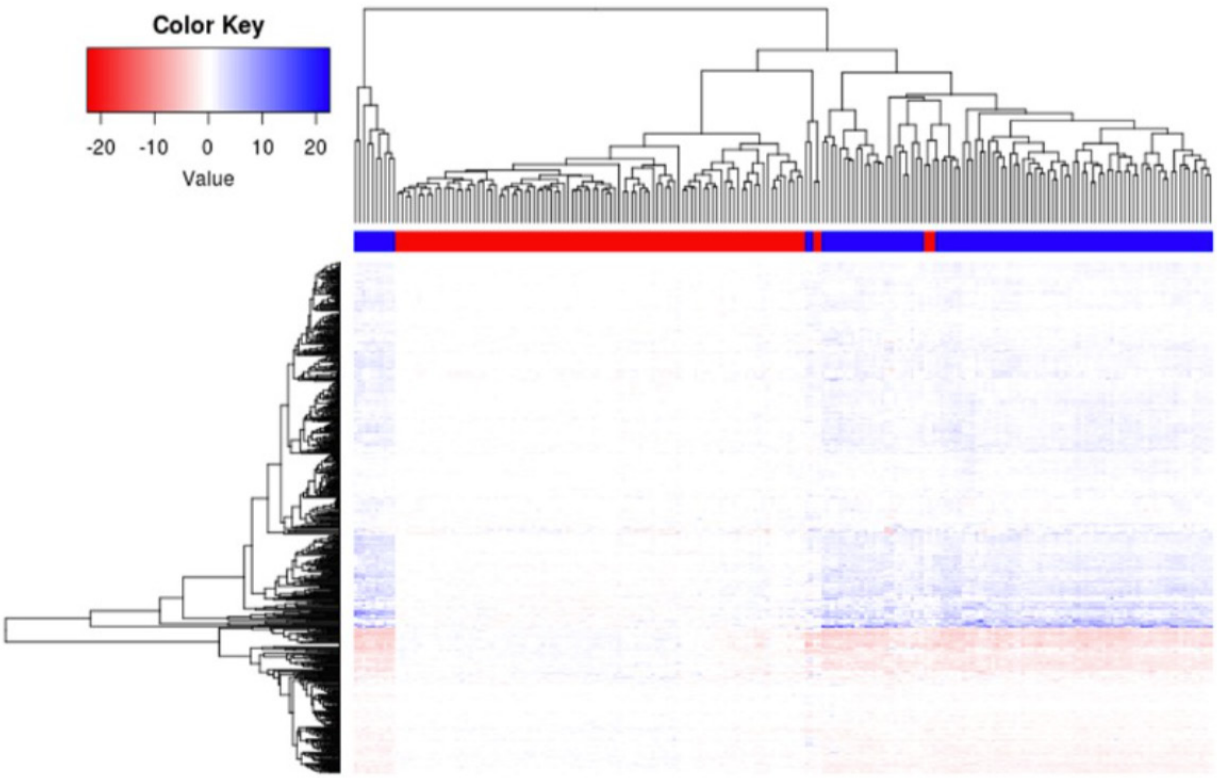

Figure 1. Clustered iPAS of dataset of clear cell renal cell carcinoma. Pathways (N=886) and samples (N=101) are clustered based on iPAS. The color scale represents the relative levels of pathway aberrance. The horizontal axis represents samples; the vertical coordinate represents deregulated pathways. iPAS means individual pathway aberrance score.

Table 1. The top ten altered pathways based on the FDR < 0.01

Category	*Term*	*p value*
REACTOME	Potassium transport channels	3.87E-80
	Proton-coupled monocarboxylate transport	6.15E-74
	Fructose catabolism	8.17E-70
	Biotin transport and metabolism	1.55E-69
	Beta oxidation of decanoyl-CoA to octanoyl-CoA-CoA	3.29E-69
	Beta oxidation of octanoyl-CoA to hexanoyl-CoA	3.29E-69
	Antigen presentation: folding	2.37E-68
	Signal transduction by L1	2.65E-68
	Vitamin B6 activation to pyridoxal phosphate	3.01E-66
	Amino acid synthesis and interconversion (transamination)	1.28E-65

FDR: false discovery rate

Validation of altered pathways

Classification capability for microarray data samples

The clustering analysis was carried out to evaluate the classification capacity for microarray data samples using the top 10 altered pathways detected by iPAS method using accumulated normal data (Figure 2). The classification efficiency for microarray data samples was calculated based on accuracy. Our iPAS method separated ccRCC from normal controls with accuracy of 0.980. In light of this result, we infer that iPAS is useful to predict marker pathways for ccRCC with high accuracy.

Changed percentage of pathway

In the current study, we computed the changed percentage of each pathway in 101 ccRCC samples. Based on the changed percentage of a special pathway in all ccRCC samples equal to 100%, a total of 5 significant pathways were extracted including proton-coupled monocarboxylate transport, antigen presentation: folding, assembly and peptide loading of class I MHC, hormone-sensitive lipase (HSL)-mediated triacylglycerol hydrolysis, chromosome maintenance, and unwinding of DNA. Significantly, these 5 pathways were a fraction of 886 altered pathways. Moreover, the gene-level statistics of 24 genes which were enriched in the pathway of antigen presentation: folding, assembly and peptide loading of class I MHC was computed, and depicted in Figure 3. From this image, we found that the gene expression levels of these genes in the ccRCC were universally disturbed relative to that in normal condition. Significantly, the alteration of the expression level of *HLA-G* was remarkably obvious.

Discussion

To gain more understanding of the molecular mechanisms underlying ccRCC, we applied a straightforward and novel pathway analysis approach to identify deregulated pathways in ccRCC, which was on the basis of the comparison of a tumor sample with the accumulated normal samples (we utilized the "reference" to refer to the accumulated normal samples). In the current study, a total of 886 altered pathways were identified in ccRCC and normal samples using T test. Among these, the most remarkably significant pathways were proton-coupled monocarboxylate transport, biotin transport and metabolism, beta oxidation of decanoyl-CoA to octanoyl-CoA-CoA, and antigen presentation: folding, assembly and peptide loading of class I MHC. Our iPAS method separated ccRCC from normal controls with accuracy of 0.98, which suggests that iPAS is useful to predict marker pathways for ccRCC with high ac-

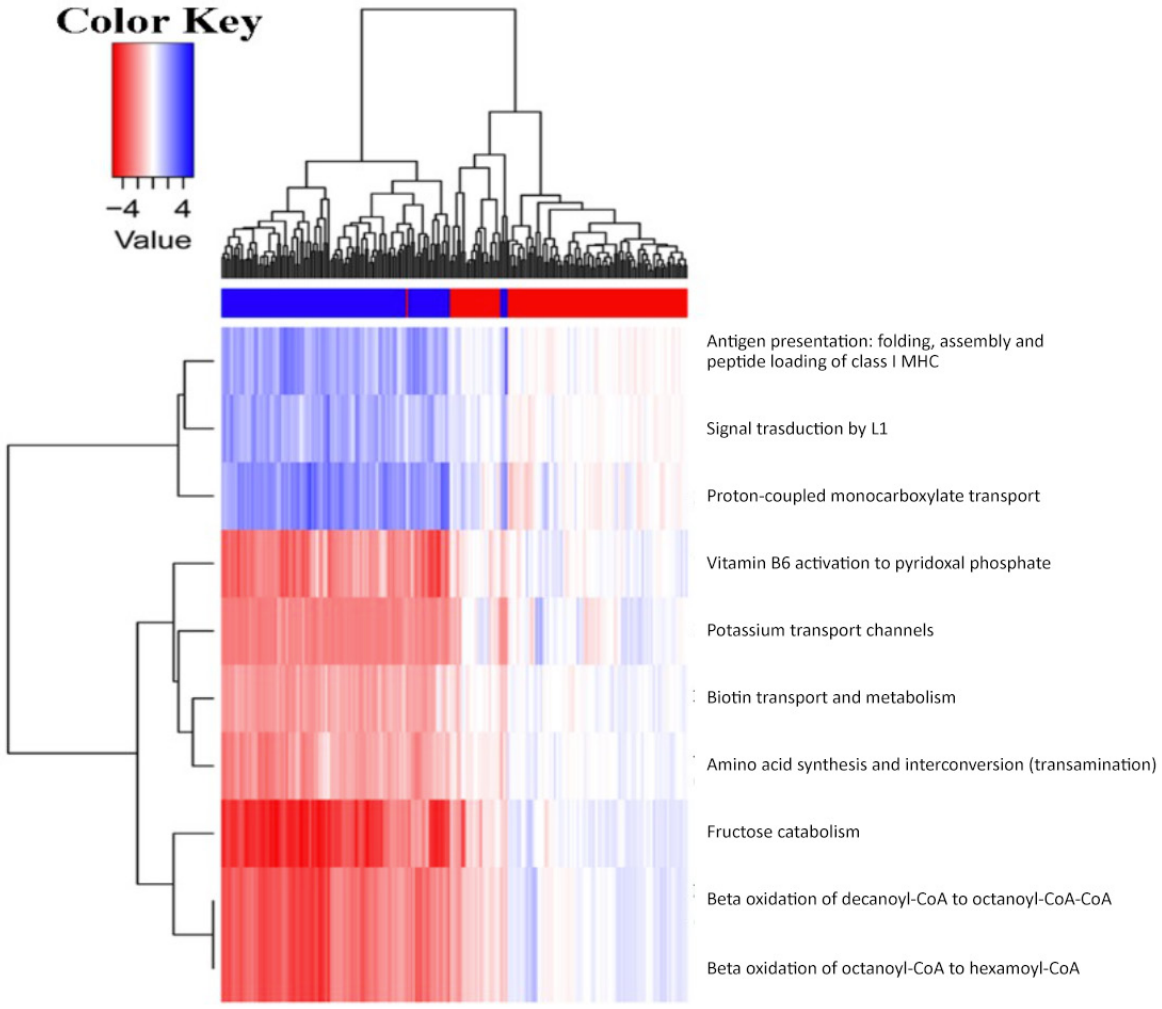

Figure 2. The cluster heat map of the top 10 pathways. The color scale represents the relative levels of pathway aberrance; the horizontal axis represents samples; the vertical coordinate represents pathways.

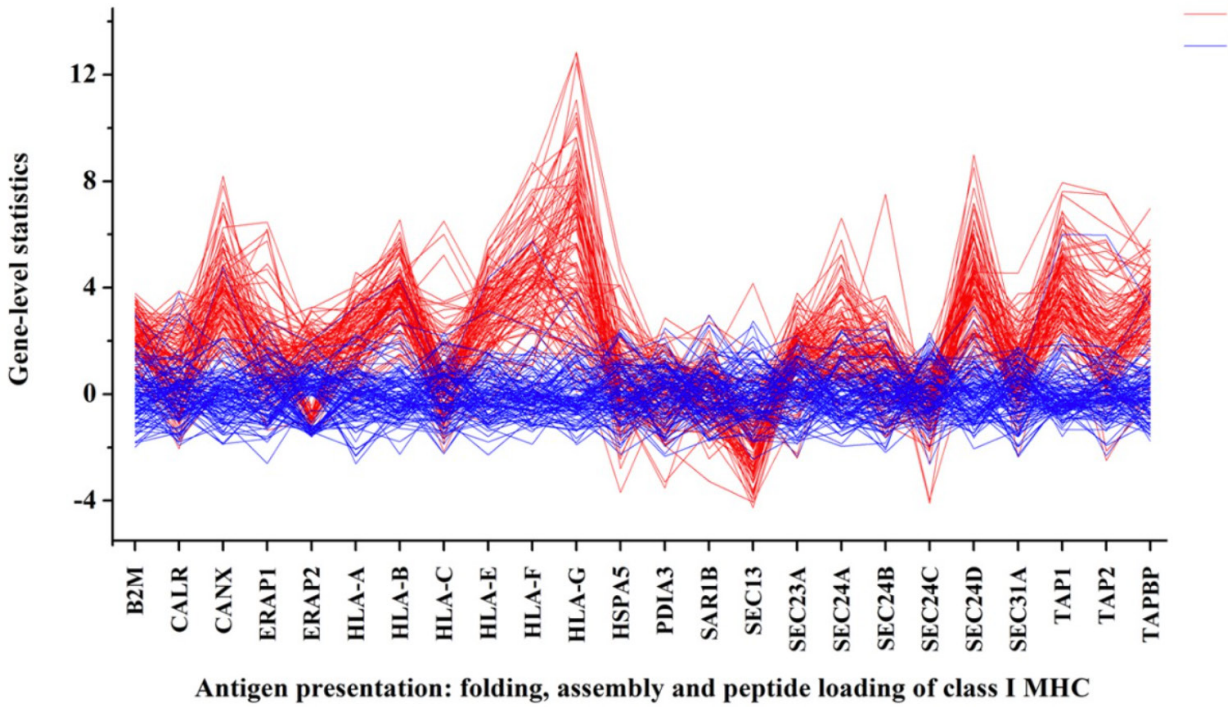

Figure 3. Expression pattern of genes in the pathway of antigen presentation: folding, assembly and peptide loading of class I MHC. Each line stands for sample (red: tumor; blue: normal).

curacy. Importantly, the pathways of proton-coupled monocarboxylate transport, antigen presentation: folding, assembly and peptide loading of class I MHC and so on were extracted based on the changed percentage =100%. Comprehensively, we found that proton-coupled monocarboxylate transport, and antigen presentation: folding, assembly and peptide loading of class I MHC were the most significant pathways.

Many important pathways are deregulated in the initiation and progression of cancer. Identification of the involved aberrant pathways in an individual was of great importance to explore patho-mechanisms and to further find new strategies for personal treatment in the future [19]. Indeed, many current methods for pathway analysis characterize the activity of a pathway for the entire samples but do not offer information on the aberrance in an individual tumor sample. With the demand for personalized interpretation of pathways, some pathway analyses have been developed to examine the individualized pathway [20,21]. PARADIGM, as an analysis tool, infers a pathway condition by using known functional structures.Moreover, PARADIGM performs better with multiple omics. However, it has less freedom of data and gene sets and needs predefined functional structure among omics objects. The personal pathway deregulation score (PDS) proposed by Drier and colleagues [20] is another method for personalized interpretation of pathways. This method performs better than PARADIGM. Unfortunately, PDS needs the entire cohort data to extract the principle curve to explain an individual pathway. Unlike the two methods mentioned above, Ahn et al. [13] have provided a straightforward and novel way that uses the Average Z method to calculate the iPAS to further identify the pathway aberrance of individual sample by comparing the expression data profile of an individual tumor sample with the accumulated normal samples. Additionally, this method is suitable for single layer omics data and expandable to interpret a patient that lacks cohort data. Previous studies have demonstrated a clear relationship between cancer and the pathway of proton-coupled monocarboxylate transport, thus we thought this pathway should be identified. In the current study, the Average Z proposed as candidate for iPAS exhibited that remarkable association of the of proton-coupled monocarboxylate transport pathway. This finding satisfies us that iPAS - by means of Average Z method - can offer the basic knowledge about cancer, and can be beneficial to identify cancer.

Glucose metabolism alteration is an important hallmark of cancer, which is referred to as Warburg effect [22]. To our knowledge, glucose

is vitally required by cancer cells, important for their growth [23]. Moreover, cancer cells convert glucose into lactate to further produce energy (ATP), even though under the state of sufficient oxygen relative to normal cells. It is noteworthy that the dependency on high levels of glycolysis is essential for the generation of ATP, which is associated with drug resistance and decreased anticancer efficiency [24]. In addition to ATP, lactate can attribute to angiogenesis which is crucial during the tumor growth and metastasis processes [25,26]. Crucially, lactate, as an anion, needs transporters to cross the cell membrane. Several reports have demonstrated that proton-coupled monocarboxylate transporters (MCTs) participate in the transport of monocarboxylic acids [27,28]. MCT1, one member of these transporters, plays important roles in the uptake of lactic acid from glycolytic cells [29], while MCT4, another member of the transporters, plays crucial roles in the efflux of lactic acid from glycolytic cells [30]. Moreover, Dhup et al. [31] have demonstrated that these MCTs, especially inhibition of MCT1, might be applied as potential new anti-cancer targets. Like most cancers, ccRCC also displays this metabolic condition to make use of glucolysis for ATP production [32]. Consistent with a previous study [33], the pathway of proton-coupled monocarboxylate transporters was universally aberrant in all the ccRCC samples relative to normal samples in our study. Accordingly, this pathway might aid the cell proliferation and survival of ccRCC through imbalanced exchange of lactate.

Another major aberrant pathway of antigen presentation: folding, assembly and peptide loading of class I MHC was identified involving 24 genes. Significantly, the alteration of the expression level of *HLA-G* was remarkably obvious among these 24 genes. MHC class I molecules exerts functions of immune surveillance by binding to $CD8^+$ T cells, and these molecules act in concert, making up the MHC class I antigen processing and presentation machinery (APM) [34,35]. Significantly, defects in the expression and function of APM components have been found in various solid tumors including RCC [36-38]. Kasajima et al. [39] have demonstrated that the down-regulation of APM is benefited for the therapy of colorectal cancer. HLA-G is one member of HLA family which is the main MHC class I molecule. Importantly, HLA-G plays a crucial role in immune surveillance [40]. HLA-G is reported to be related with high risk of many cancers via involving the cell-mediated immune responses [41,42]. Accordingly, the pathway of antigen presentation: folding, assembly and peptide loading of class I MHC might exert crucial functions in ccRCC progression, probably by regulating the immune response.

We applied personalized-based pathway analysis through introducing the concept of comparing an individual tumor with many accumulated normal samples. The clinical importance of this method is that it is able to explain a cancer case in a single patient. Based on the results, we showed that proton-coupled monocarboxylate transport and antigen presentation: folding, assembly and peptide loading of class I MHC were the significant pathways for ccRCC. However, the validation using other datasets would be conducted to demonstrate that these pathways are useful in classifying ccRCC and normal sample.

References

1. White NM, Yousef GM. MicroRNAs: exploring a new dimension in the pathogenesis of kidney cancer. BMC Medicine 2010;8:65.
2. Siegel R, Ma J, Zou Z, Jemal A. Cancer statistics, 2014. CA Cancer J Clin 2014;64:9-29.
3. Cheville JC, Lohse CM, Zincke H, Weaver AL, Blute ML. Comparisons of outcome and prognostic features among histologic subtypes of renal cell carcinoma. Am J Surg Pathol 2003;27:612-624.
4. Gudbjartsson T, Hardarson S, Petursdottir V, Thoroddsen A, Magnusson J, Einarsson GV. Histological subtyping and nuclear grading of renal cell carcinoma and their implications for survival: a retrospective nation-wide study of 629 patients. Eur Urol 2005;48:593-600.
5. Coppin C, Kollmannsberger C, Le L, Porzsolt F, Wilt TJ. Targeted therapy for advanced renal cell cancer (RCC): a Cochrane systematic review of published randomised trials. BJU Int 2011;108:1556-1563.
6. Parkin DM, Pisani P, Lopez AD, Masuyer E. At least one in seven cases of cancer is caused by smoking. Global estimates for 1985. Int J Cancer 1994;59:494-504.

7. Cohen HT, McGovern FJ. Renal-cell carcinoma. New Engl J Med 2005;353:2477-2490.
8. Zubac DP, Bostad L, Kihl B, Seidal T, Wentzel-Larsen T, Haukaas SA. The expression of thrombospondin-1 and p53 in clear cell renal cell carcinoma: its relationship to angiogenesis, cell proliferation and cancer specific survival. J Urol 2009;182:2144-2149.
9. Bilim V, Kawasaki T, Katagiri A, Wakatsuki SJ, Takahashi K, Tomita Y. Altered expression of β-catenin in renal cell cancer and transitional cell cancer with the absence of β-catenin gene mutations. Clin Cancer Res 2000;6:460-466.
10. Pantuck AJ, Zeng G, Belldegrun AS, Figlin RA. Pathobiology, prognosis, and targeted therapy for renal cell carcinoma: exploiting the hypoxia-induced pathway. Clin Cancer Res 2003;9:4641-4652.
11. Pei X, Li M, Zhan J et al. Enhanced IMP3 Expression Activates NF-κB Pathway and Promotes Renal Cell Carcinoma Progression. PLos One 2015; Ee0124338.
12. Wozniak MB, Le Calvez-Kelm F, Abedi-Ardekani B et al. Integrative genome-wide gene expression profiling of clear cell renal cell carcinoma in Czech Republic and in the United States. PLoS One 2013;8:e57886.
13. Ahn T, Lee E, Huh N, Park T. Personalized identification of altered pathways in cancer using accumulated normal tissue data. Bioinformatics 2014;30:i422-i429.
14. Brazma A, Parkinson H, Sarkans U et al. ArrayExpress--a public repository for microarray gene expression data at the EBI. Nucleic Acids Res 2003;31:68-71.
15. Croft D, O'Kelly G, Wu G et al. Reactome: a database of reactions, pathways and biological processes. Nucleic Acids Res 2011;39:D691-697.
16. Irizarry R A, Hobbs B, Collin F et al. Exploration, normalization, and summaries of high density oligonucleotide array probe level data. Biostatistics 2003;4:249-264.
17. Perez-Llamas C, Lopez-Bigas N. Gitools: analysis and visualisation of genomic data using interactive heatmaps. PLoS One 2011;6:e19541.
18. Mohammadi A, Saraee MH, Salehi M. Identification of disease-causing genes using microarray data mining and Gene Ontology. BMC Med Genom 2011;4:12.
19. Khatri P, Sirota M, Butte AJ. Ten years of pathway analysis: current approaches and outstanding challenges. PLoS Comput Biol 2012;8:e1002375.
20. Drier Y, Sheffer M, Domany E. Pathway-based personalized analysis of cancer. Proc Natl Acad Sci 2013;110:6388-6393.
21. Vaske CJ, Benz SC, Sanborn JZ et al. Inference of patient-specific pathway activities from multi-dimensional cancer genomics data using PARADIGM. Bioinformatics 2010;26:i237-i245.
22. Icard P, Lincet H. A global view of the biochemical pathways involved in the regulation of the metabolism of cancer cells. Biochim Biophys Acta (BBA)-Reviews on Cancer 2012;1826:423-433.
23. Munoz-Pinedo C, El Mjiyad N, Ricci J. Cancer metabolism: current perspectives and future directions. Cell Death Dis 2012;3:e248.
24. Vaske CJ, Benz SC, Sanborn JZ et al. Overcoming trastuzumab resistance in breast cancer by targeting dysregulated glucose metabolism. Cancer Res 2011;71:4585-4597.
25. Hunt TK, Aslam R, Hussain Z, Beckert S. Lactate, with oxygen, incites angiogenesis. Adv Exp Med Biol 2008;614:73-80.
26. Folkman J. Angiogenesis in cancer, vascular, rheumatoid and other disease. Nat Med 1995;1:27-31.
27. Halestrap AP, Wilson MC. The monocarboxylate transporter family--role and regulation. Iubmb Life 2011;64:109-119.
28. Halestrap AP, Meredith D. The SLC16 gene family—from monocarboxylate transporters (MCTs) to aromatic amino acid transporters and beyond. Pflug Arch Eur J Phy 2004;447:619-628.
29. Sonveaux P, Végran F, Schroeder T et al. Targeting lactate-fueled respiration selectively kills hypoxic tumor cells in mice. J Clin Invest 2008;118:3930-3942.
30. Whitaker-Menezes D, Martinez-Outschoorn UE, Lin Z et al. Evidence for a stromal-epithelial "lactate shuttle" in human tumors: MCT4 is a marker of oxidative stress in cancer-associated fibroblasts. Cell Cycle 2011;10:1772-1783.
31. Dhup S, Kumar Dadhich R, Ettore Porporato P, Sonveaux P. Multiple biological activities of lactic acid in cancer: influences on tumor growth, angiogenesis and metastasis. Curr Pharm Design 2012;18:1319-1330.
32. Langbein S, Frederiks WM, zur Hausen A et al. Metastasis is promoted by a bioenergetic switch: new targets for progressive renal cell cancer. Int J Cancer 2008;122:2422-2428.
33. Pinheiro C, Longatto-Filho A, Ferreira L et al. Increasing expression of monocarboxylate transporters 1 and 4 along progression to invasive cervical carcinoma. Int J Gynecol Pathol 2008;27:568-574.
34. Jensen PE. Recent advances in antigen processing and presentation. Nat Immunol 2007;8:1041-1048.
35. Yewdell JW. The seven dirty little secrets of major histocompatibility complex class I antigen processing. Immunol Rev 2005;207:8-18.
36. Leone P, Shin EC, Perosa F, Vacca A, Dammacco F, Racanelli V. MHC Class I Antigen Processing and Presenting Machinery: Organization, Function, and Defects in Tumor Cells. J Natl Cancer Inst 2013;105:1172-1187.
37. Lorenzi S, Forloni M, Cifaldi L et al. IRF1 and NF-kB restore MHC class I-restricted tumor antigen processing and presentation to cytotoxic T cells in aggressive neuroblastoma. PloS One 2012;7:135-139.
38. Seliger B, Atkins D, Bock M et al. Characterization of human lymphocyte antigen class I antigen-processing machinery defects in renal cell carcinoma lesions with special emphasis on transporter-associated with antigen-processing down-regulation. Clin Cancer Res 2003;9:1721-1727.
39. Kasajima A, Sers C, Sasano H et al. Down-regulation of the antigen processing machinery is linked to a loss of inflammatory response in colorectal cancer. Hum Pathol 2010;41:1758-1769.
40. Cavallo F, De Giovanni C, Nanni P, Forni G, Lollini PL. 2011: the immune hallmarks of cancer. Cancer Immu-

nol Immunother 2011;60:319-326.

41. Silva ID, Muniz YCN, Sousa MCPS et al. HLA-G 3' UTR polymorphisms in high grade and invasive cervico-vaginal cancer. Hum Immunol 2013;74:452-458.
42. Wischhusen J, Waschbisch A, Wiendl H. Immune-refractory cancers and their little helpers—An extended role for immunetolerogenic MHC molecules HLA-G and HLA-E? Semin Cancer Biol 2007;17:459-468.